Enhanced visualization of choroidal vessels using ultrahigh resolution ophthalmic OCT at 1050 nm

B. Považay, K. Bizheva, B. Hermann, A. Unterhuber, H. Sattmann, A.F. Fercher and W. Drexler

Department of Medical Physics, Christian Doppler Laboratory, University of Vienna, A-1090 Vienna, Austria
Wolfgang.Drexler@univie.ac.at

C. Schubert and P.K. Ahnelt

Department of Physiology, University of Vienna, A-1090 Vienna, Austria

M. Mei and R. Holzwarth

MenloSystems GmbH, am Klopferspitz 19, 82152 Martinsried, Germany

W. J. Wadsworth, J.C. Knight, P. St. J. Russel

Department of Physics, University of Bath, Bath BA2 7AY, United Kingdom

Abstract: In this article the ability of ultrahigh resolution ophthalmic optical coherence tomography (OCT) to image small choroidal blood vessels below the highly reflective and absorbing retinal pigment epithelium is demonstrated for the first time. A new light source (λ_c= 1050 nm, $\Delta\lambda$ = 165 nm, P_{out}= 10 mW), based on a photonic crystal fiber pumped by a compact, self-starting Ti:Al_2O_3 laser has therefore been developed. *Ex-vivo* ultrahigh resolution OCT images of freshly excised pig retinas acquired with this light source demonstrate enhanced penetration into the choroid and better visualization of choroidal vessels as compared to tomograms acquired with a state-of-the art Ti:Al_2O_3 laser (Femtolasers Compact Pro, λ_c= 780 nm, $\Delta\lambda$= 160 nm, P_{out}= 400 mW), normally used in clinical studies for *in vivo* ultrahigh resolution ophthalmic OCT imaging. These results were also compared with retinal tomograms acquired with a novel, spectrally broadened fiber laser (MenloSystems, λ_c= 1350 nm, $\Delta\lambda$= 470 nm, P_{out} = 4 mW) permitting even greater penetration in the choroid. Due to high water absorption at longer wavelengths retinal OCT imaging at ~1300 nm may find applications in animal ophthalmic studies. Detection and follow-up of choroidal neovascularization improves early diagnosis of many retinal pathologies, e.g. age-related macular degeneration or diabetic retinopathy and can aid development of novel therapy approaches.

OCIS codes: (170.4500) Optical coherence tomography; (170.3880) Medical and biological imaging; (170.1650) Coherence imaging

References and links

1. D. Huang, E.A. Swanson, C.P. Lin, J.S. Schuman, W.G. Stinson, W. Chang, M.R. Hee, T. Flotte, K. Gregory, C.A. Puliafito, J.G. Fujimoto, "Optical coherence tomography," Science **254**, 1178-1181 (1991).
2. B. Bouma and J. Tearney (ed) *Handbook of Optical Coherence Tomography* (Marcel Dekker Inc., 2002).
3. A.F. Fercher, "Optical coherence tomography," J. Biomed. Opt. **1**, 157-173 (1996).
4. C.A Puliafito, M.R. Hee, J.S. Schuman, J.G. Fujimoto *Optical coherence tomography of ocular disease* (Thorofare, New Jersey: Slack Inc., 1995).
5. W. Drexler, U. Morgner, R.K. Ghanta, J.S. Schuman, F. Kärtner, J.G. Fujimoto, "Ultrahigh-resolution ophthalmic optical coherence tomography, " Nature Medicine **7**, 502-507 (2001).

#2460 - $15.00 US Received May 07, 2003; Revised August 11, 2003

6. W. Drexler, H. Sattmann, B. Hermann, T.H. Ko, M. Stur, A. Unterhuber, C. Scholda, O. Findl, M. Wirtitsch, J.G. Fujimoto, A.F. Fercher, "Enhanced visualization of macula pathology using ultrahigh resolution optical coherence tomography, " Arch Ophthalmol-Chic **121**, 695-706 (2003).
7. M.E. Boulton, F. Docchio, P. Dayhaw-Barker, R. Ramponi, R. Cubeddu, "Age-related changes in the morphology, absorption and fluorescence of melanosomes and lipofuscin granules of the retinal pigment epithelium," Vision Res. **30**, 1291 (1990).
8. Schmitt, S.H. Xiang, K.M. Yung, "Differential absorption imaging with optical coherence tomography," J.Opt. Soc. Am. A, **15**, 2288-2297 (1998).
9. G. M. Hale, M. R. Querry, "Optical constants of water in the 200 nm to 200 µm wavelength region," Appl. Opt. **12**, 555-563 (1973).
10. ANSI Standard Z136.1-2000.
11. Y. Wang, J. Nelson, Z. Chen, B. Reiser, R.S. Chuck, R. S. Windeler, „Optimal wavelength for ultra-high resolution optical coherence tomography," Opt. Express **11**, 1411-1417 (2003).
12. B. Považay, K. Bizheva, A. Unterhuber, B. Herman, H. Sattmann, A. Fercher, W. Drexler, A. Apolonski, W.J. Wadsworth, J. C. Knight, P.St.J. Russel, M. Vetterlein, E. Scherzer, "Sub-micrometer resolution optical coherence tomography," Opt. Lett. **27**, 1800-18024 (2002).
13. A. Apolonski, B. Považay, A. Unterhuber, T.A Birks, W.J. Wadsworth, P.St.J. Russel, W. Drexler, "Spectral shaping of supercontinuum in a cobweb photonic-crystal fiber with sub-20-fs pulses," J.Opt.Soc.Am. B **19**, 2165-2170 (2002).
14. K. Bizheva, B. Považay, B. Hermann, H. Sattmann, W. Drexler, M. Mei, R. Holzwarth, T. Hoelzenbein, V. Wacheck, H. Pehamberger, "Compact, broad bandwidth fiber laser for sub-2 µm axial resolution optical coherence tomography in the 1300 nm wavelength region," Opt. Lett. **28**, 707-709 (2003).
15. I. Hartl, X.D. Li, C. Chudoba, R. K. Ghanta, T.H. Ko, J. G. Fujimoto, J. K. Ranka and R.S. Windeler, "Ultrahigh resolution optical coherence tomography using continuum generation in an air-silica microsctructure optical fiber," Opt. Lett. **26**, 608-610 (2001).
16. A. Roggan, M. Friebel, K. Dörschel, A. Hahn and G. Müller, „Optical properties of circullating human blood in the wavelength range 400-2500 nm," J. Biomed. Opt. **4,** 36-46 (1999).
17. Q. Li, A.M Timmers, K. Hunter, C. Gonzalez-Pola, A.S. Lewin, D.H Reitze, W.W Hauswirth, "Noninvasive imaging by optical coherence tomography to monitor retinal degeneration in the mouse," Invest. Ophthalmol. Vis. Sci. **42**, 2981-2989 (2001).
18. N.M. Bressler, S.B. Bressler, E.S. Gragoudas, "Clinical characteristics of choroidal neovascular membranes," Arch Ophthalmol **105,** 209-213 (1987).
19. L. M. Aiello *Principles and practice of ophthalmology: clinical practice* (Saunders, Philadelphia, PA, 1994).

Introduction

Optical coherence tomography is an imaging technique that permits retrieval of cross-sectional morphological and functional information from superficial regions of biological tissue[1-3]. Since ocular media are essentially transparent in the visible and near-infrared wavelength region, and provide optical access to the anterior eye segment and retina, OCT was initially applied to ophthalmology[4]. Recently, an ultrahigh resolution version of ophthalmic OCT has been developed to enable *in vivo* optical biopsy of the retina, i.e., visualization of all major intraretinal layers, comparable to the quality achieved with conventional histopathology[5,6]. Figure 1 shows a typical *in-vivo* ultrahigh resolution OCT image of a human fovea with areolar atrophy, associated with foveomacular dystrophy, acquired with a state of the art broad bandwidth (~150 nm) Ti:Al_2O_3 laser, centered at ~800 nm that enables ~3 µm axial resolution in the *in vivo* tomogram of the retina. The tomogram was obtained with a fiber based OCT system interfaced to a fundus camera[6] and demonstrates the ability of ultrahigh resolution ophthalmic OCT to visualize all major intraretinal layers. The tomogram also shows that in the parafoveal area (Fig. 1, solid arrows) where the retinal pigment epithelium (RPE) layer is intact, OCT is able to resolve only a very superficial region of the underlying choriocapillaris and choroid, due to strong backscattering and absorption of light by melanin in the RPE. However, in the central foveal region (Fig. 1, dotted arrow) where RPE atrophy is present the reduced amount of pigment permits greater penetration into the choroid and therefore enhanced visualization of vessels positioned deeper in the choroid.

Early stages of development of many retinal pathologies such as proliferative diabetic retinopathy (PDR) and age related macular degeneration (AMD) are accompanied by choroidal neovascularizaiton, i.e. extensive growth of new blood vessels in the choroid and the retina. Therefore, detection of the onset of choroidal neovascularization and periodic

#2460 - $15.00 US Received May 07, 2003; Revised August 11, 2003

monitoring of its development over time can provide a valuable insight to ophthalmologists and may permit earlier and better diagnostics of retinal pathologies, as well as assignment of a therapy at the very early stages of a disease when it is most favorably treatable. In addition, it can aid development and evaluation of novel therapeutic approaches.

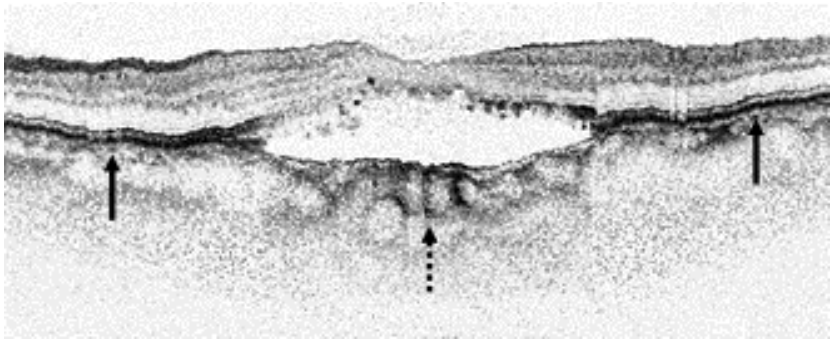

Fig. 1. *In-vivo* ultrahigh resolution OCT image (2700 x 830 pixels, 5 mm x 2 mm) of human retina with areolar atrophy associated with foveomacular dystrophy, acquired with the Ti:Al_2O_3 light source. Solid arrows indicate intact RPE; dashed arrow indicates RPE with atrophy enabling visualization of choroidal vessels.

As demonstrated in Fig. 1, ophthalmic ultrahigh resolution OCT operating in the ~800 nm wavelength range does not provide sufficient access to the choroid when the RPE layer is intact. Considering that absorption of light from melanin, the major chromophore in the RPE, decreases monotonically with increasing wavelength[7], and that in general scattering of light in biological tissues exhibits a similar trend[8], it is expected that OCT operating at longer wavelengths than 800 nm may be able to image morphological features deeper in the choroid. However, a major limitation to *in-vivo* ophthalmic OCT imaging at wavelengths much longer than 800 nm is posed by the light absorption properties of water[9], since the vitreous contains ~90% water and the average human eye length is ~25 mm. The water absorption profile has a local minimum at ~1060 nm (μ_a ~0.013 mm^{-1} at λ = 1060 nm, as compared to μ_a ~0.002 mm^{-1} at λ = 800 nm) and a second one at ~ 1300 nm (μ_a ~0.1 mm^{-1} at λ = 1300 nm), meaning that power losses due to water absorption will be 48% at 1060 nm and 99.3% at ~1300 nm as compared to 10% at ~800 nm for a double pass of the optical beam through a human eye. This will result in relative sensitivity loss of 2.4 dB when imaging at ~1060 nm and 21 dB at ~1300 nm. However, according to the ANSI standard[10], the maximum permissible light exposure in the eye increases with wavelength and is ~5 mW at both λ~1060 nm and λ~1300 nm as compared to ~1.5 mW at λ ~800 nm, calculated for 10 s continuous wave exposure. Thus by using higher incident power at longer wavelengths the sensitivity of ophthalmic OCT is improved by 5.2 dB. In addition, a recent study has shown that imaging biological tissue at central wavelengths close to 1000 nm provides the advantage of minimal OCT axial resolution degradation resulting from water dispersion in soft tissues[11].

Consequently, sufficiently powerful broad bandwidth light sources centered at λ~1060 nm have great potential for ophthalmic OCT in clinical investigations, while sources emitting at λ~1300 nm may prove useful for animal model studies (with significantly smaller eye length, e.g., mouse and rat).

To evaluate the image penetration depth of ultrahigh resolution ophthalmic OCT into the choroid at longer wavelengths relative to the penetration achieved with a state of the art Ti:Al_2O_3 laser centered at ~800 nm, we have developed a photonic crystal fiber (PCF) based light source emitting at ~1050 nm, and also used a novel, compact, broad bandwidth fiber laser centered at ~1350 nm. Since fiber optical components designed to support propagation of broad bandwidth light in the 1000 nm wavelength region are not readily available, we have

#2460 - $15.00 US Received May 07, 2003; Revised August 11, 2003

chosen to test our hypothesis by using a free space OCT system and to acquire preliminary retinal tomograms *ex-vivo*. For proper comparison, all three light sources were interfaced to the free space OCT system, previously described in detail[12] and specifically modified to support propagation of broad bandwidth light in the wavelength ranges from 600 nm to 1000 nm and from 900 nm to 1600 nm with minimal power and spectral losses. Custom designed achromatic lenses (5 mm diameter, 10 mm focal length) operating in the specified wavelength ranges with minimal chromatic aberrations were used in the OCT system. The beam diameter produced by all three light sources was large enough to fill in the imaging lenses in order to achieve high lateral OCT resolution.

Methods

A PCF (provided by the University of Bath) with 1,9 µm core size and 24 mm length was pumped with the output of a self-starting Ti:Al_2O_3 laser (Femtolasers Produktions GmbH, λ_c = 790 nm, $\Delta\lambda$ = 33 nm, P_{out} = 300 mW), to generate a broad bandwidth spectrum, covering a local minimum in the water absorption spectrum located at ~1060 nm. High NA (0.8 and 0.6) achromatic microscope objectives were employed to couple the oscillator output into the PCF and to collimate the generated output. A chirped-mirror pre-compressor compensated the dispersion introduced by the optical components before the fiber. Since the shape and spectral width of the generated supercontinuum are polarization sensitive[13], the polarization state of the input beam was controlled by quarter- and half- wave plates.

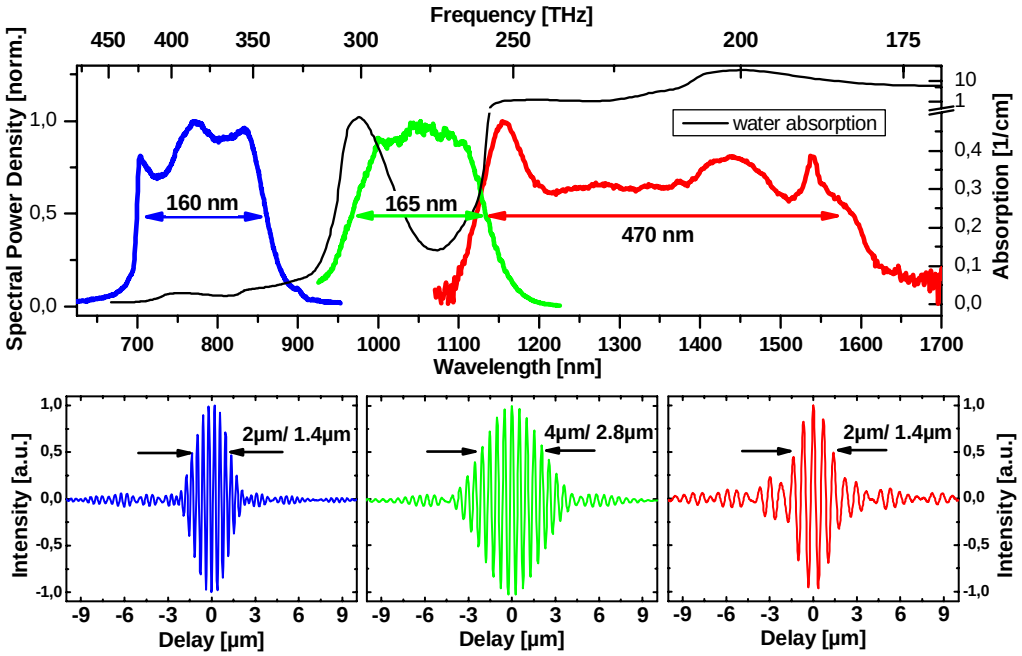

Fig. 2. Output spectra (top): Ti:Al_2O_3 (blue line), PCF based source (green line) and fiber laser based light source (red line), overlaid with water absorption spectrum (black line). Corresponding fringe patterns produced by interfacing the light sources to the OCT system (bottom).

The PCF generated supercontinuum, spanning from 400 nm to 1200 nm at the pedestal, with P_{out} = 60 mW was filtered with a long pass filter to produce a Gaussian shaped spectrum with 165 nm full width of half maximum and P_{out} = 10 mW (Fig. 2, top, green line). The long term stability of this spectrum generated at the longer wavelength side of the pump spectrum was limited by long term walk off due to thermal changes which influenced the beam pointing at the input coupler of the fiber. However, this slow decay resulted mainly in a loss of spectral

#2460 - $15.00 US
Received May 07, 2003; Revised August 11, 2003

bandwidth (9 nm loss in ~ 40 min), as well as an even slower power loss at the fiber output. Free space resolution of 3.5 µm x 4 µm (lateral x axial), corresponding to 2.5 µm x 3 µm in tissue and 98 dB sensitivity at 2 mW incident power was achieved by interfacing the PCF based source to the OCT system (Fig. 2 bottom, green line).

In addition, a novel broad bandwidth, compact fiber laser based light source[14] (MenloSystems, spectral range 1100 nm – 1700 nm, P_{out} = 45 mW) was used for retinal OCT imaging in the 1350 nm wavelength region, where the water absorption spectrum has another local minimum. Compared to other nonlinear fiber based light sources centered at 1300 nm[15] the Menlo Systems fiber laser offers a much broader bandwidth, is more stable, compact and user friendly. Due to a 12 dB spectral modulation at ~ 1550 nm, a short pass filter was used to block the spectrum beyond 1650 nm. The filtered output was centered at 1375 nm, with a spectral bandwidth of 470 nm and P_{out} = 4 mW (Fig. 2, top, red line). Resolution of 4.5 µm x 2 µm in air, corresponding to 3 µm x 1.4 µm in tissue and 95 dB sensitivity at 0.5 mW incident power (Fig. 2 bottom, red line) was achieved by coupling the fiber laser to the OCT system.

For the purpose of comparison, ultrahigh resolution OCT tomograms of pig retinas were also acquired with a state of the art Ti:Al_2O_3 laser (Fig. 2 top, blue line) operating in the 800nm wavelength region (Femtolasers Compact Pro, λ_c = 780 nm, $\Delta\lambda$ = 160 nm, P_{out} = 400 mW). By interfacing the Ti:Al_2O_3 source to the OCT system, free space resolution of 2.5 µm x 2 µm (lateral x axial), corresponding to 2 µm x 1.4 µm in biological tissue and 105 dB sensitivity at 5 mW incident power was achieved (Fig. 2 bottom, blue line).

Because post mortem retinal tissue quickly looses optical quality due to cell degradation, and human retinas are not readily available, freshly excised pig retinas were used in the present study. The pig eye, a well-established animal model in retinal physiology research, closely resembles the morphology of human retina, except for the lack of a fovea. Eyes were enucleated from anesthetized domestic pigs and immersed in buffered saline (PBS, pH 7.4). Within 30 minutes post mortem the cornea, lens, and vitreous were removed to prevent loss of transverse image resolution due to ocular aberrations in an intact eye. Strips (~10 mm x 10 mm) were excised from the remaining eyecup in the area of the optical disc and placed in a chamber with buffer solution to prevent dehydration. OCT tomograms were acquired through an optical window (~160 µm thick glass coverslip) in the chamber.

Pig retinas were imaged *ex-vivo* with ultrahigh resolution OCT within 1-3 hours after excision, before changes in the retinal tissue morphology and optical properties became noticable. Since imaging with the three light sources necessitated changes in the detector and optics system to optimize the performance of the OCT instrument at each wavelength region, tomograms were acquired from different retinal samples. To properly compare the OCT image penetration depth in retinal tissue at different wavelengths, retinal samples with similar pigmentation, excised from the same animal race were imaged at similar locations.

Results and discussion

The *ex-vivo* pig retina tomogram (Fig. 3 top, 2000 x 1000 pixels, 2 mm x 1 mm, ~1.5 minutes image acquisition time), acquired with the Ti:Al_2O_3 laser demonstrates that ultrahigh resolution OCT in the 800 nm wavelength region permits detailed visualization of intra-retinal layers. However, access to the choroid is restricted to shallow depths even for high incident power (5 mW, 105 dB sensitivity), permitting observation of only superficial depths in the choroid. In comparison, the pig retina tomogram acquired with the PCF based light source (Fig. 3 middle, 2000 x 1010 pixels, 2 mm x 1 mm, ~1.5 minutes acquisition time) shows better penetration in the choroid (blood vessels positioned one above the other are observed), despite the fact that the tissue was imaged with lower incident power and sensitivity (2 mW, 98 dB). Superior penetration in the choroid was achieved with the MenloSystems fiber laser as demonstrated in the retinal tomogram in Fig. 3, bottom (2000 x 888 pixels, 2 mm x 1 mm, ~1.5 minutes acquisition time). Though the image was acquired with much lower incident power of 0.5 mW and sensitivity of only 95 dB, a group of interlaced vessels is clearly visualized. Moreover, the vessel walls are more distinctly outlined and the overall image

#2460 - $15.00 US Received May 07, 2003; Revised August 11, 2003

contrast in the choroid appears to be better. The images in Fig. 3 confirm the expected improvement in OCT image penetration in retinal choroid at longer wavelengths, most probably due to a decrease in light absorption and scattering from melanin.

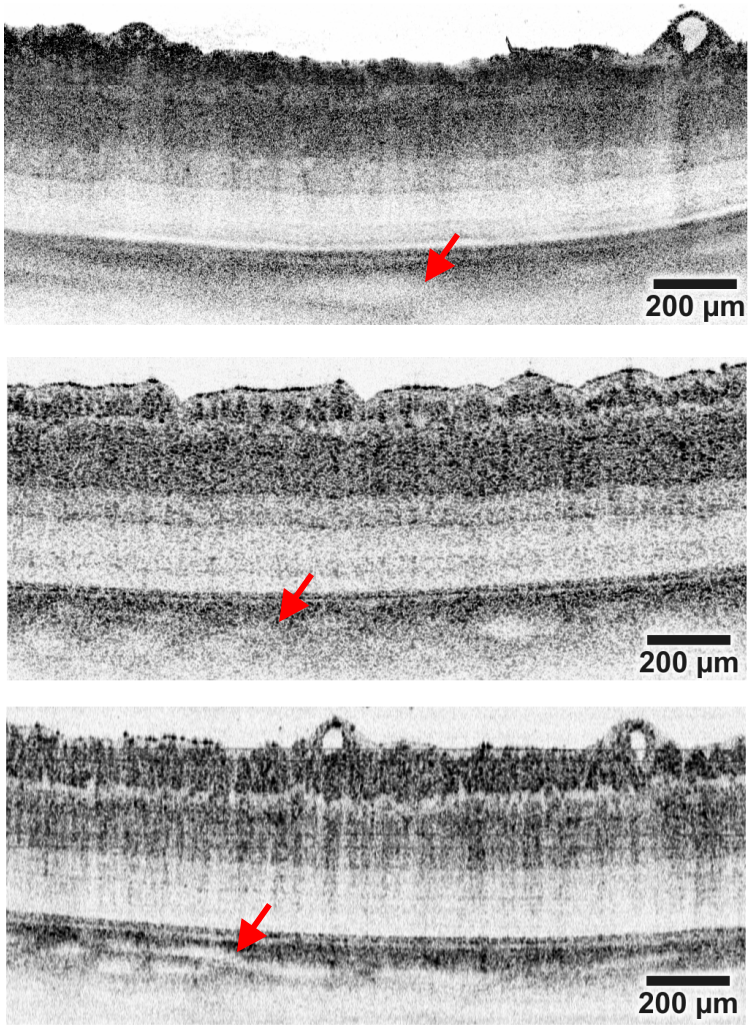

Fig. 3. *Ex-vivo* OCT images of pig retinas, acquired with the Ti:Al_2O_3 source (top, at ~800 nm, SNR 105 dB, 2000 x 1000 pixels, 2 x 1 mm), PCF based source (middle, at ~1050 nm, SNR 98 dB, 2000 x 1010 pixels, 2 x 1 mm), and the fiber laser based source (bottom, at ~1350 nm, SNR 95 dB, 2000 x 888 pixels, 2 x 1 mm). Red arrows indicate choroidal blood vessels.

As mentioned above, the axial OCT resolution achieved with the PCF based light source in tissue is ~3 µm as compared to ~1.4 µm achieved with both the Ti:Al_2O_3 laser (λ_c~800 nm) and the MenloSystems fiber laser (λ_c~1350 nm). However, the retinal image shown in Fig. 4 acquired *ex-vivo* with the PCF based source demonstrates that the OCT spatial resolution is sufficient to resolve the highly reflective surfaces of the RPE, as well as to provide distinct visualization of the major intraretinal layers. The red arrow marks a region in the image corresponding to the choroid, where cross-sections of multiple small blood vessels positioned above each other are clearly visible. The stacked choroidal vessels also appear to be partially filled with coagulated blood. Since all OCT tomograms presented in this paper were acquired *ex-vivo*, the effect of blood flow on the ability of OCT to image stacked vessels in the choroid

#2460 - $15.00 US
Received May 07, 2003; Revised August 11, 2003

has not been investigated so far. Considering the fact that light scattering from blood cells decreases with increasing wavelength[16], it is expected that the visibility of stacked blood vessels will improve at longer wavelengths due to the reduced light extinction in retinal tissue.

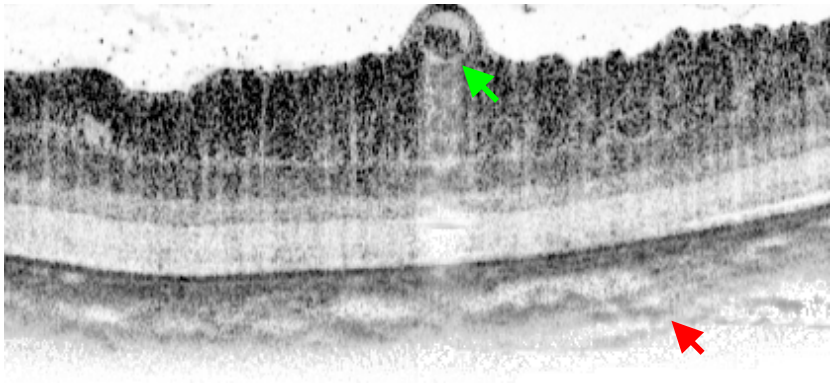

Fig. 4. *Ex-vivo* OCT image of a pig retina, acquired with the PCF based source at ~1050 nm (2000 x 1010 pixels, 2 mm x 1 mm). The red arrow marks a region in the choroid, where multiple small blood vessels partially filled with coagulated blood, positioned on top of each other are visible. Green arrow depicts a blood vessel on the retinal surface with reduced shadowing because of better penetration at the imaging wavelength.

Conclusion

We have developed a broad bandwidth light source centered at λ_c~1050 nm and have employed a novel fiber laser based source at λ_c~1350 nm to evaluate the ophthalmic ultrahigh resolution OCT image penetration depth in choroidal tissue at longer wavelengths. Superior penetration into the choroid was realized with the fiber laser based light source (MenloSystems, λ_c~1350 nm), though due to strong water absorption at longer wavelengths and the large axial length of a human eye (~25 mm), this light source is not applicable for *in-vivo* imaging of human retina. However, the fiber laser may find clinical applications for *in-vivo* imaging of the anterior segment of a human eye. It can also be applied successfully in ophthalmic animal studies[17] since the eye length of a mouse is ~5 mm, thus reducing the optical power losses arising from water absorption from 21 dB (in human eye) to 4.3 dB (in mouse eye) for a double pass of the optical beam. Compared to opthalmic ultrahigh resolution OCT tomograms acquired at λ_c~800 nm, better visualization of the choriocapillaris and choroid was achieved with the PCF based source (λ_c~1050 nm). When used with a fiber based ultrahigh resolution OCT system and interfaced to a fundus camera, this light source has great potential for clinical applications for monitoring choroidal neovascularization, associated with AMD and diabetic retinopathy[18-19]. In addition imaging at longer wavelengths may permit *in-vivo* measurement of blood flow in choroidal vessels simultaneously with the acquisition of the morphological tomograms by using functional OCT techniques.

Acknowledgements

We gratefully acknowledge the Department of Experimental Animal Research, Vienna University and the Department of Veterinary Pathology, Veterinary University for providing us with samples of retinal tissue, and also the contributions of A. Stingl and T. Le from Femtolasers Produktions GmbH and the technical assistance of L. Schachinger, Vienna University. This work was supported in part by FWF P14218-PSY, FWF Y 159-PAT, EC Grant OLK6CT200100279, CRAF-1999-70549, Femtolasers Produktions GmbH and the Christian Doppler Society.